Sphingomyelin/Phosphatidylcholine/Cholesterol Phase Diagram: Boundaries and Composition of Lipid Rafts

Rodrigo F. M. de Almeida, Aleksandre Fedorov, and Manuel Prieto
Centro de Química-Física Molecular, Instituto Superior Técnico, Universidade Técnica de Lisboa, Lisbon, Portugal

ABSTRACT The ternary system palmitoylsphingomyelin (PSM)/palmitoyloleoylphosphatidylcholine (POPC)/cholesterol is used to model lipid rafts. The phase behavior of the three binary systems PSM/POPC, PSM/cholesterol, and POPC/cholesterol is first experimentally determined. Phase coexistence boundaries are then determined for ternary mixtures at room temperature (23°C) and the ternary phase diagram at that temperature is obtained. From the diagram at 23°C and the binary phase diagrams, a reasonable expectation is drawn for the ternary phase diagram at 37°C. Several photophysical methodologies are employed that do not involve detergent extraction, in addition to literature data (e.g., differential scanning calorimetry) and thermodynamic rules. For the ternary phase diagrams, some tie-lines are calculated, including the one that contains the PSM/POPC/ cholesterol 1:1:1 mixture, which is often used in model raft studies. The diagrams here described are used to rationalize literature results, some of them apparently discrepant, and to discuss lipid rafts within the framework of liquid-ordered/liquid-disordered phase coexistence.

INTRODUCTION

When the model for lipid rafts was proposed (Simons and Ikonen, 1997), there was already the awareness that the detergent resistant membranes (DRM) isolated from cells were probably liquid ordered (lo) domains, based on the fact that liposomes with resistance to Triton X-100 (TX100) solubilization are in ordered phases (gel or solid ordered (so) and lo), whereas in the liquid disordered (ld) phase (phospholipid fluid phase) they are solubilized (Schroeder et al., 1994). An additional important result was that the resistance of proteins to solubilization correlated with the lipid phase of the membrane where the protein was inserted (Schroeder et al., 1994, 1998). In sum, not only lipid-lipid interactions suffice to make a DRM, but also the insolubility of some proteins is probably conferred by the fact that they localize preferentially to ordered domains.

On the other hand, it was known that the DRM isolated from membranes were enriched in (glyco)sphingolipids and cholesterol (chol) and depleted in phosphatidylcholines (PC) (Simons and Ikonen, 1997). The natural lipids with highest main transition temperature (T_m) in membranes are (glyco)-sphingolipids, some of them having T_m much higher than 37°C (e.g., cerebrosides (Marsh, 1990)) but in principle their abundance is too low to form stable gel domains. In fact, whereas natural PC have mostly unsaturated acyl chains, in the case of (glyco)sphingolipids there is a high abundance of very long and/or saturated chains (Marsh, 1990). These results led to the design of experiments involving model membranes with (at least) three components: a low T_m lipid (usually a PC), a high T_m lipid (a saturated PC or a sphingolipid), and chol (e.g., Silvius, 1992; Silvius et al., 1996; Ahmed et al., 1997; Xu and London, 2000). The main conclusions from such experiments can be summarized as follows: from detergent independent methods, it is known that chol can promote phase separation between a low T_m lipid and a high T_m lipid at an intermediate temperature when the fraction of one lipid is too low to phase separate in the absence of chol. The results have been interpreted as separation of an ld and an lo phase, the first one being rich in the low T_m lipid and depleted in the high T_m lipid and chol, and the opposite for the other phase. At very high chol concentrations, the bilayer tends to form a unique lo phase. Above T_m of both lipids, phase separation can persist. The rationalization presented for these phenomena is a preferential interaction of chol with (mostly) saturated lipids. This is supported by the fact that other sterols, which are unable to increase the order of the bilayer, antagonize phase separation at gel/fluid coexistence conditions. Recently, more systematic detergent extraction studies have revealed surprising results, namely that for many liposome compositions, solubilization is easier at 4°C than at 37°C and that some glycosphingolipids facilitate solubilization (Sot et al., 2002). It should be kept in mind, though, that these results would have to be rationalized in the context of a quaternary phase diagram. Recent results from NMR spectroscopy and calorimetric techniques suggest that TX100 can promote the formation of new or stabilize lo domains by segregating together with the ld major components (Heerklotz, 2002).

Silvius et al. (1996) alerted to the fact that results on high $T_m$lipid/low $T_m$lipid/chol could be rationalized within a ternary phase diagram, but much of the recent information in the literature is still reported in a descriptive manner. Even for binary systems PC/chol, the most studied being 1,2-dipalmitoyl-*sn*-glycerophosphocholine (DPPC)/chol, there are several phase diagrams differing significantly among themselves (e.g., Vist and Davis, 1990; Lentz et al., 1980; McMullen and McElhaney, 1995). This disagreement is probably related to the similarities of physical properties in the

Submitted March 26, 2003, and accepted for publication June 19, 2003.

Address reprint requests to Manuel Prieto, Centro de Química-Física Molecular, Complexo I, IST, Av. Rovisco Pais, 1049-001 Lisbon, Portugal. Tel: 351-218419219; Fax: 351-218464455; E-mail: prieto@alfa.ist.utl.pt.

0006-3495/03/10/2406/11 $2.00

lo and ld phases, which makes it difficult to differentiate between them (London and Brown, 2000). For instance, phase separation in 1,2-dioleoyl-*sn*-glycerophosphocholine (DOPC)/*N*-palmitoyl-D-sphingomyelin (PSM)/chol systems is difficult to detect by atomic force microscopy (AFM) because there is little height difference between the two phases, but the domains can be visible as differences in the packing density (Yuan et al., 2002). Only with the addition of the ganglioside GM1 the visualization of domains as height differences was clear. The usual methods to study the phase behavior of two-component membranes are much more difficult to apply to the study of ternary membranes, especially when one of the components is cholesterol (Silvius, 1992).

Recently, a ternary phase diagram was published for the system 1,2-dilauroyl-*sn*-glycerophosphocholine/1,2-distearoyl-*sn*-glycerophosphocholine/chol based on information from microscopy and fluorescence resonance energy transfer (FRET) (Feigenson and Buboltz, 2001). However, as mentioned by the authors, a more relevant system would be sphingomyelin (SM)/1-palmitoyl,2-oleoyl-*sn*-glycerophosphocholine (POPC)/chol.

The purpose of the present work is to describe the phase behavior of a typical DRM-containing lipid mixture used recurrently in the literature by methods that do not involve detergent extraction. In this way, fluorescence techniques have been applied to mixtures of PSM, POPC, and chol in different proportions. Partial binary phase diagrams were determined for PSM/POPC (so/ld phase separation), POPC/chol (ld/lo phase separation), and PSM/chol (ld/lo and so/lo phase separation). The ternary phase diagrams PSM/POPC/chol (ld/lo, ld/so, lo/so, and ld/lo/so phase separation) at room temperature (23°C) and at 37°C (physiological temperature) were then obtained, and they were used to rationalize published data on these systems. In addition, the tie-lines obtained are particularly important because they give the composition and fraction of the coexisting ld/lo phases. The phase diagrams here obtained are the simplest models that explain the results obtained by us and others and that are, at the same time, thermodynamically consistent. It is also worth mentioning that the phase diagrams do not contain information about phase domain size, shape, and dynamics.

MATERIALS AND METHODS

Chemicals

POPC was purchased from Avanti Polar Lipids (Alabaster, AL). PSM, chol, and 5-doxyl stearic acid (5-NS) were purchased from Sigma-Aldrich (Steinheim, Germany). Diphenylhexatriene (DPH) and *trans*-parinaric acid (*t*-PnA) were obtained from Molecular Probes (Leiden, The Netherlands).

Liposome preparation

Multilamellar vesicles (MLV) containing the appropriate lipids and DPH when used were prepared by standard procedures (e.g., Mateo et al., 1993). The suspension medium was sodium phosphate 10 mM, NaCl 150 mM, EDTA 0.1 mM buffer (pH 7.4). The samples were kept overnight at 4°C and all the measurements started at the lower temperature, at which the demixing process is faster (de Almeida et al., 2002). The heating rate was always below 0.2°C/min. *t*-PnA and 5-NS were added from stock solutions (ethanol and methanol, respectively) to the MLV suspension. The samples were re-equilibrated by freeze-thaw cycles and incubation above T_m (Sklar et al., 1977a; Santos et al., 1998; Yuann and Morse, 1999). The samples were slowly brought to 4°C for 90 min and then slowly heated to the measurement temperature and incubated for 1 h. Measurements on random samples were repeated for longer incubation times and this did not affect the results.

The probe/lipid ratios used were 1/200 for DPH and 1/500 for *t*-PnA. The quencher/lipid ratio was 1/25 (based on a gel phase membrane/aqueous phase partition coefficient $K_p = 12{,}570$ (Wardlaw et al., 1987) and for a total lipid concentration of 0.2 mM).

PSM and POPC concentration in stock solutions were confirmed by phosphorus analysis (McClare, 1971). Probe concentrations were determined spectrophotometrically using ε(*t*-PnA, 299.4 nm, ethanol) = $89 \times 10^3\ M^{-1}cm^{-1}$ (Sklar et al., 1977b) and ε(DPH, 355 nm, chloroform) = $80.6 \times 10^3\ M^{-1}cm^{-1}$ (Lentz, 1988).

Absorption and fluorescence measurements and data analysis

The instrumentation was the same as previously described (de Almeida et al., 2002). The temperature (±0.2°C within replicates) was achieved by a Julabo F25 circulating water bath and was controlled with 0.1°C precision directly inside the cuvette with a Pt100.

For steady-state measurements with DPH, samples were excited at 358 nm and emission collected at 430 nm. For anisotropy measurements (e.g., Lakowicz, 1999), 1 cm × 0.4 cm cuvettes were used and for intensity (as well as time-resolved) measurements, 0.5 cm × 0.5 cm cuvettes were used.

For time-resolved measurements with DPH, excitation wavelength was 340 nm (laser of 4-dicyanomethylene-2-methyl-6-(*p*-dimethylaminostyryl)-4*H*-pyran) and the emission was collected at 430 nm. For *t*-PnA, excitation and emission wavelengths were 303 nm (laser of rhodamine 6G) and 405 nm, respectively. For details on fluorescence decay analysis, see, e.g., de Almeida et al. (2002).

The lifetime-weighted quantum yield is defined by (Lakowicz, 1999)

$$\bar{\tau} = \sum_i \alpha_i \tau_i \tag{1}$$

and the mean or average fluorescence lifetime is given by

$$\langle \tau \rangle = \left(\sum_i \alpha_i \tau_i^2 \right) \Big/ \left(\sum_i \alpha_i \tau_i \right) \tag{2}$$

for a decay described by a sum of exponentials, where α_i is the normalized pre-exponential and τ_i the lifetime of the decay component *i*. Two or three exponentials were required to describe DPH decays, whereas three or four were necessary for *t*-PnA.

The lifetime and the fraction of light associated with each component are in very good agreement with the literature for DPH (Lentz, 1988) and *t*-PnA (Mateo et al., 1993; Sklar et al., 1977a).

Phase coexistence boundaries determination

Different methodologies were used for determining phase boundaries, which will be briefly described.

When there is phase separation into phase 1 and phase 2, the probe distributes between the two phases, and the fraction of probe in phase i, P_i, depends on the amount of each phase (fraction X_i) and the partition coefficient. In this situation, from the Weber's law of additivity of anisotropy (e.g., Lakowicz, 1999), the steady-state anisotropy of a probe in a lipidic system where phase separation occurs is given by

$$\langle r \rangle = \frac{\varepsilon_1 P_1 \Phi_1 g_1 \langle r \rangle_1 + \varepsilon_2 P_2 \Phi_2 g_2 \langle r \rangle_2}{\varepsilon_1 P_1 \Phi_1 g_1 + \varepsilon_2 P_2 \Phi_2 g_2}, \tag{3}$$

where ε_i is the molar absorption coefficient, Φ_i is the quantum yield, and g_i is the fluorescence intensity at the emission wavelength in a normalized spectrum for pure phase i. Usually, $\varepsilon_1 = \varepsilon_2$, and if there are no shifts in the emission, $g_1 = g_2$. If the partition coefficient of the probe is close to 1 and the variation of quantum yield is negligible, then a linear relationship between $\langle r \rangle$ and X_i is obtained. According to the lever rule, X_i and the mole fraction of component j x_j are linearly related; thus, in the two-phase coexistence range, a representation of $\langle r \rangle$ versus x_j should be a straight line. The probe DPH obeys (in a reasonable degree) the conditions necessary for that to hold.

In the case of lifetime-weighted quantum yield, because of the proportionality to the fluorescence quantum yield, the following relationship is valid,

$$\bar{\tau} = P_1\bar{\tau}_1 + P_2\bar{\tau}_2, \quad (4)$$

for a probe distributed by two phases 1 and 2. In the case of a partition coefficient close to 1, $\bar{\tau}$ is linearly related to x_j. This is the case for *t*-PnA distributed by ld/lo phases (Mateo et al., 1993). In this way, $\langle r \rangle_{DPH}$ and $\bar{\tau}_{t\text{-PnA}}$ can be used to detect ld/lo phase coexistence regions in a very direct and correct way. One further advantage is that both $\bar{\tau}$ and $\langle r \rangle$ are independent of probe concentration, eliminating this source of uncertainty (as compared, e.g., with steady-state fluorescence intensity). It is also important to note that both $\langle r \rangle$ and $\bar{\tau}$ are sensitive only to the microenvironment of the probe; thus they are independent of the domain size, in opposition to other methodologies, e.g., FRET (Loura et al., 2001).

The variation of $\langle r \rangle_{DPH}$ (Lentz et al., 1976a, 1976b) (and other linear probes, derived from DPH or PnA (Sklar et al., 1979)) with temperature is a well-established method to determine phase diagrams (gel/fluid coexistence region) of binary phospholipid membranes. In fact, the onset and completion of the lateral phase-separation are identified as breaks in the temperature dependence of a property characteristic of the lipid state (Lentz et al., 1976b). Nevertheless, due to particularities of the system under study, extra care was taken as described in the Results section, in a similar way to that described by Sklar et al. (1979).

The quenching of DPH fluorescence by spin-labeled fatty acids can be used to study phase separation (e.g., Ahmed et al., 1997; Xu and London, 2000). The probe shows no preference for any of the phases, and the spin-labeled fatty acid (in the present case, 5NS) due to the bulky nitroxide moiety, partitions preferentially to the fluid phase. In this way, when there is so/lo phase separation, the quenching of DPH fluorescence by 5-NS is less efficient than when only one phase is present. Besides partitioning, there may also be an effect arising from interfaces (5-NS may tend to accumulate in the defects between domains of the two phases). In the present study, the quenching was evaluated by I/I_0 or $\bar{\tau}/\bar{\tau}_0$ versus chol mole fraction, where I is the steady-state fluorescence intensity and the index 0 means absence of quencher. It is expected that either I/I_0 or $\bar{\tau}/\bar{\tau}_0$ have an initial plateau, changing to higher values when phase separation occurs, and decreasing back to a lower level when a one-phase situation is reached again.

In the present work, all the phase coexistence boundaries were determined from photophysical data (fluorescence anisotropy, lifetime, and quenching) of two probes both with fluorescence lifetimes in the nanosecond time range. In this way, there is internal consistence, i.e., all the involved processes (fluorescence and anisotropy) and interactions (quenching) happen during the probes lifetime, which is similar. Certainly that, when using other spectroscopic techniques such as resonance spectroscopies, different time (and so length) scales sampled by the probes are involved, and the boundaries will shift, although not in a critical way, from those here presented. Later in the manuscript, we will comment on the differences between published binary phase diagrams.

RESULTS

PSM/POPC binary system

For PSM/POPC binary phospholipid mixtures, the method used to determine the phase diagram was the variation of $\langle r \rangle_{DPH}$ with temperature (Fig. 1). In the case of pure POPC vesicles, with a main-transition temperature T_m of (-2.9 ± 1.3)°C (Koynova and Caffrey, 1998), all the data shown correspond to the ld phase, and so it is clear that there is a significant variation in the values of $\langle r \rangle_{DPH}$ even for the same phase (e.g., at 3°C, $\langle r \rangle \sim 0.20$, and at 60°C, $\langle r \rangle \sim 0.05$). In the case of pure PSM vesicles, comparing the curve obtained with DSC thermograms (typical peaks with maximum at ~41.4°C (Koynova and Caffrey, 1995; Marsh, 1990) and a width at half-height of no more than 4°C (Maulik and Shipley, 1996; Epand and Moscarello, 1982) it can be seen that there is: i), a very good agreement between the calorimetric maximum and the midpoint of the transition detected by $\langle r \rangle_{DPH}$, validating this methodology, and ii), an artificial broadening of the transition (in other words, near the T_m, there is a gradual variation of $\langle r \rangle_{DPH}$ with temperature). Comparing the curves for 100 and 75 mol% PSM, it can also be seen that the values, e.g., at higher temperatures (100% fluid) are composition dependent. All these effects were considered for the calculation of the PSM/POPC phase diagram. The correction of Mabrey and Sturtevant (1976) was applied to the mixed composition vesicles, allowing for a 1.8°C width for pure POPC (Curatolo et al., 1985) once that the two acyl chains are different. For PSM, a width of 3.1°C was considered once this is not strictly a pure component (Maulik and Shipley, 1996).

The PSM/POPC phase diagram (Fig. 2) is clearly one of a nonideal mixture, with a broad gel/fluid phase separation region, and due to the horizontal part of the solidus boundary, gel-gel phase separation must occur. There is also the suggestion of a fluid-fluid phase separation above the liquidus line in the region of high x_{PSM}. For pure PSM, the data from Maulik and Shipley (1996) is presented (the value for T_m is the same as the one recovered from our data in Fig. 1, but as described the width of the transition is much less).

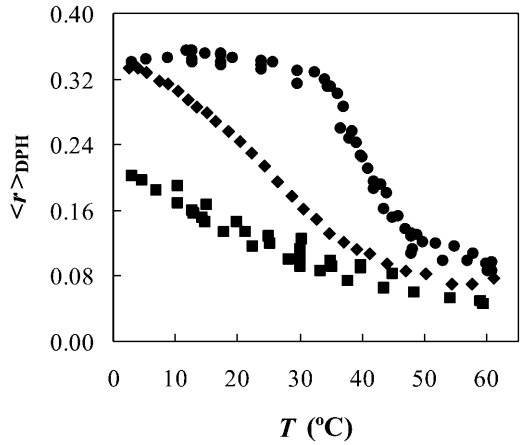

FIGURE 1 Determination of solid ordered (so)/liquid disordered (ld) phase coexistence boundaries. Steady-state anisotropy of DPH ($\langle r \rangle_{DPH}$) as a function of temperature for MLV composed of 100% PSM (*circles*), 75 mol % PSM/25 mol % POPC (*diamonds*), and 100% POPC (*squares*).

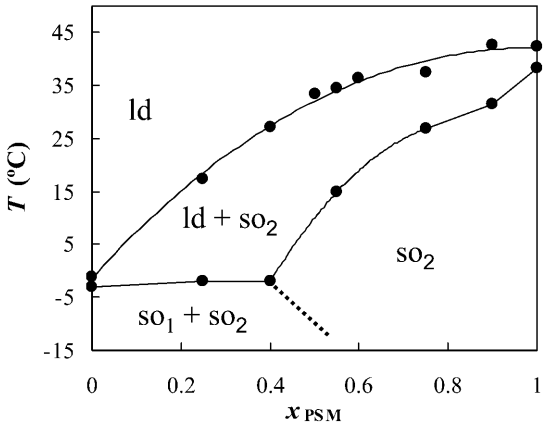

FIGURE 2 Phase diagram for PSM/POPC MLV. Experimental data are shown as circles. The dotted line is hypothetical. The point for pure POPC is from Curatolo et al. (1985). It is considered that there are one ld phase and two so phases (so_1 rich in POPC and so_2 rich in PSM).

PSM/chol binary system

Above the T_m of PSM, the lo/ld phase boundaries were determined from the variation of $\langle r \rangle_{DPH}$ with x_{chol}. A typical result is shown in Fig. 3 for PSM/chol lipid mixtures at 50°C. The three straight lines distinguish the three regimes: only ld phase for low chol mol fraction (x_{chol}); ld/lo coexistence for intermediate x_{chol} and only lo phase for high x_{chol}. The fluorescence decays of DPH in this system were also obtained. Interestingly, although the variation of the lifetimes was at most by a factor of 1.5, preventing a good determination of the phase boundaries (Fig. 3 *C*), the phase boundaries determined from the anisotropies (Fig. 3 *A*) coincide with special points in the trend of the amplitudes of the decay components (Fig. 3 *B*). This is in further support to the phase boundaries from $\langle r \rangle$ data.

The phase diagram for PSM/chol is presented in Fig. 4. For bovine brain SM/chol, a partial phase diagram is reported above the T_m of SM, with an ld/lo phase separation region (Sankaram and Thompson, 1990) which compares well with the same region of the diagram presented here (especially when taking the higher x_{chol} in the error bars presented in that phase diagram).

Below the T_m of PSM, where the presence of cholesterol should induce the formation of an lo phase from an so phase (Ipsen et al., 1987; Ahmed et al., 1997), the addition of 50 mol % chol did not affect significantly the anisotropy of DPH. Besides, the $\bar{\tau}$ of both DPH and *t*-PnA suffered only minor changes. For DPH, this is not so surprising, but for *t*-PnA it is an unusual result. In fact, the long component of *t*-PnA, which can be considered as a ''fingerprint'' for the so lipid phase, was practically the same in the absence and in the presence of 50 mol % cholesterol (~35–40 ns at 18°C, a value typical of a DPPC gel (Mateo et al., 1993; Sklar et al., 1977a)). Nevertheless, the amplitude of the long component was below 5%, and the $\bar{\tau}$ values were typical of fluid even in the absence of chol below the T_m (Mateo et al., 1993; Sklar et al., 1977a). These results, on one side, point to particularities in the structure and/or dynamics of the PSM lamellar phases, and on the other hand prevent the use of those fluorescence parameters to determine the so/lo phase boundaries.

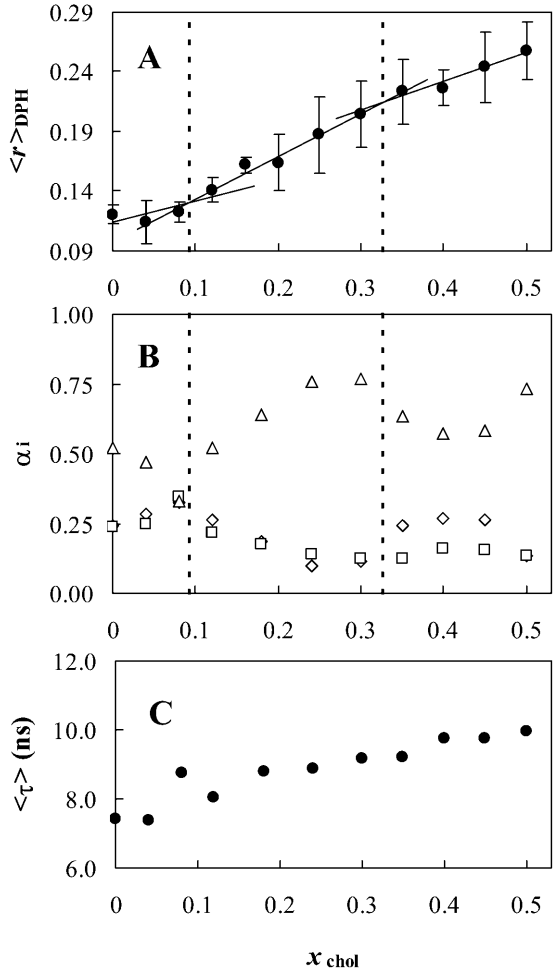

FIGURE 3 Determination of ld/liquid ordered (lo) phase coexistence boundaries for the PSM/cholesterol (chol) lipid mixtures at 50°C determined from the $\langle r \rangle_{DPH}$ (*A*). The three straight lines distinguish the three regimes: only ld phase for low chol mol fraction (x_{chol}), ld/lo coexistence for intermediate x_{chol}, and only lo phase for high x_{chol}. The amplitudes of the fluorescence decay components of DPH (short component, *diamonds*: (0.4 ± 0.1) ns; intermediate component, *squares*: (3.4 ± 1.2) ns; long component, *triangles*: (9.6 ± 1.4) ns) are also shown (*B*) together with the phase boundaries determined from the anisotropy data. DPH mean fluorescence lifetime versus chol mol fraction (*C*) is fairly constant.

These fluorescence data can raise doubt about the formation of an lo phase. However, differential scanning calorimetry (DSC) results show a decrease in the enthalpy of the transition with two regimes, and the enthalpy becomes zero for ~42–50 mol % chol (Maulik and Shipley, 1996; Calhoun and Shipley, 1979). In addition, x-ray diffraction data show that the lamellar spacing increases with chol above T_m and decreases below T_m becoming the same at high x_{chol} (Maulik and Shipley, 1996). All these are characteristic features of the formation of an lo phase. In fact, calorimetric

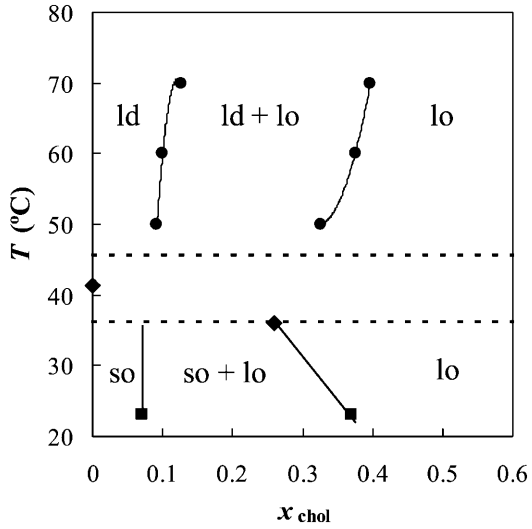

FIGURE 4 PSM/chol phase diagram. The points shown were determined from $\langle r \rangle_{DPH}$ (*circles*), DPH quenching by 5-NS (*squares*), and literature (*diamonds*, see text for details). Between the dotted lines is the regime of strong $\langle r \rangle_{DPH}$ variation for pure PSM.

data for PSM/chol displays the same qualitative features as the data for DPPC/chol (Estep et al., 1979). Thus, it is expected that the phase diagram has the same shape for both these systems (except for the fact that there seems to be no pretransition for PSM (Maulik and Shipley, 1996; Barenholz et al., 1976)).

The so/lo phase boundaries at room temperature were determined using the quenching of DPH fluorescence by 5-NS as described under Materials and Methods.

In the phase diagram for the system PSM/chol presented in Fig. 4, the different regions are the same as in other phospholipid/chol phase diagrams (binary monotectic systems) where the presence of the sterol induces the formation of a new fluid phase, the lo phase (Ipsen et al., 1987), but both the so/lo and the ld/lo phase coexistence regions are broader, i.e., the composition of the lo phase boundary is located at higher x_{chol} values. The point for pure PSM is the maximum of the DSC peak (Marsh, 1990; Epand and Moscarello, 1982; Maulik and Shipley, 1996), which corresponds to the midpoint of the transition detected by $\langle r \rangle_{DPH}$ versus T (see Figs. 1 and 2). Another point ($x_{chol} = 0.26$; $T = 36°C$) is the fraction of chol at which the two enthalpy regimes cross (Maulik and Shipley, 1996) and the temperature to which the sharp peak decreases in the presence of chol (Estep et al., 1979). This is taken as the point above and to the right of which there is no more so phase.

The phase diagram presented here is also consistent with the appearance of a resolvable broad endotherm on DSC scans for x_{chol} ~0.10 (Estep et al., 1979).

POPC/chol binary system

The ld/lo phase coexistence for the system POPC/chol was studied by means of $\langle r \rangle_{DPH}$ and $\bar{\tau}_{t\text{-PnA}}$ versus x_{chol}. No determinations were made below the T_m of POPC, i.e., so/lo phase boundaries. The results obtained from the two methodologies were essentially the same. The partial phase diagram is shown in Fig. 5, where a broad ld/lo coexistence region can be observed. The phase diagram is similar to the previous published one (Mateo et al., 1993), except that for the lower temperatures, the phase coexistence both begins and ends at slightly higher x_{chol} values.

PSM/POPC/chol ternary system

To build the ternary phase diagram at 23°C, the following information was used: the binary tie-lines at 23°C (and the expected ternary phase behavior from the binary phase diagrams (Rhines, 1956)), thermodynamic principles (the phase rule, and limitations to the two-phase/one-phase boundaries imposed by the Gibbs energy minimum principle (Rhines, 1956)), and the phase behavior of similar systems (Silvius et al., 1996).

Furthermore, experimental data was obtained for ternary mixtures at 23°C out of the three-phase region (tie-triangle, see below) to avoid further complexity. For low x_{PSM} (ld/lo coexistence), $\langle r \rangle_{DPH}$ was used, whereas for low x_{POPC} (so/lo coexistence), the methodology based on the quenching of DPH by 5-NS was applied. At low x_{PSM} (ld/lo coexistence), the tie-lines should have a direction close to the direction of the left side of the diagram, and for low x_{POPC} (so/lo coexistence), their direction should be approximate to that of the right side of the diagram. Concomitantly, the measurements were performed at constant x_{PSM} and x_{POPC}, respectively. In this way, the determination of phase coexistence boundaries is performed approximately along a tie-line. An example is given in Fig. 6, where quenching methodology results are presented. The final diagram, drawn taking into consideration all the aspects mentioned above, is shown in Fig. 7 *A*. The main features of the diagram are a broad lo/ld phase coexistence region on the left side of the diagram (high POPC/PSM ratio), a considerable so/lo phase

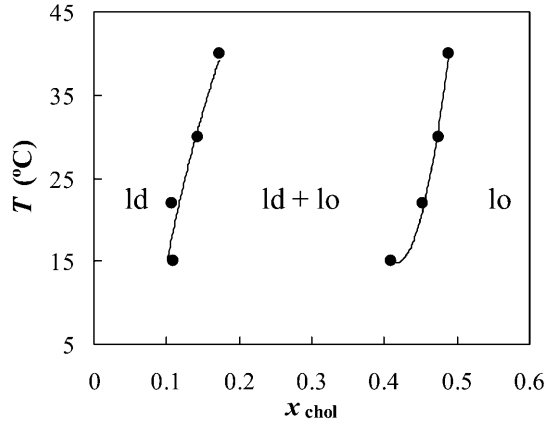

FIGURE 5 POPC/chol phase diagram. The experimental points were determined from $\langle r \rangle_{DPH}$ and *t*-PnA lifetime.

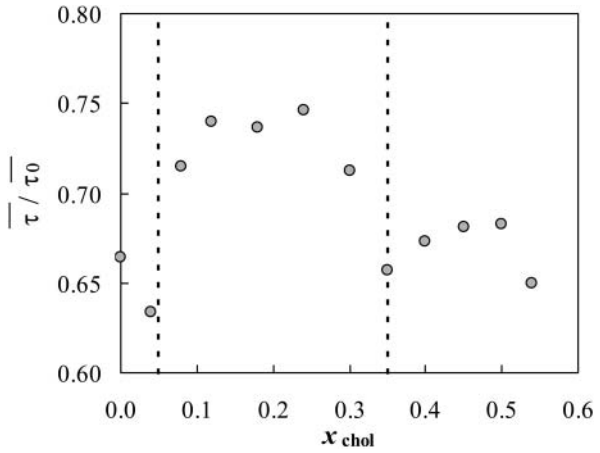

FIGURE 6 Determination of so/lo phase coexistence boundaries. The lipid mixtures contain 15 mol % of POPC and varying proportions of PSM and chol, at 23°C. The method is based on the quenching of DPH fluorescence by 5-NS observed as a decrease in the lifetime of the fluorophore. The dotted lines separate the high quenching efficiency (one phase (so for low x_{chol}, lo for high x_{chol})) from the low quenching efficiency (so/lo coexistence and segregation of probe and quencher, for intermediate x_{chol}).

coexistence region and the presence of a tie-triangle, i.e., a region of three-phase coexistence, where the composition of each phase is given by the position of each corner of the triangle and where the lever rule is valid. The sides of the tie-triangle can be considered tie-lines, once that the third phase is present only in an infinitesimal amount. In Fig. 7 *B*, the phase diagram at 37°C is shown. The same data was used as for the diagram at 23°C, except that no experimental points were determined for ternary compositions. The boundaries at 37°C are very difficult to determine, and one of the reasons is that $\langle r \rangle_{DPH}$ is on the strongly temperature-dependent region of PSM transition, and so the meaning of the results is difficult to assess.

Nevertheless, it suggests an interesting behavior, as will be apparent in the Discussion section. The so/lo coexistence region is much smaller than at 23°C, and concomitantly the lo/ld (the ''raft region'') is much broader.

In Table 1, the extremes of the tie-lines highlighted in Fig. 7, *A* and *B*, are given. These points describe the rafts composition (lo phase) and also the ld composition.

DISCUSSION

PSM was chosen to represent the high-melting component for several reasons. First of all, an SM isolated from natural sources was ruled out due to the complex thermotropic behavior (e.g., Barenholz et al., 1976) and acyl chain composition (Marsh, 1990). On another hand, C16:0 is one of the fatty acids that comprise the bulk of the fatty acid residues found in SM isolated from natural sources (Estep et al., 1979). Finally, PSM has a simple thermotropic behavior, but nevertheless with a T_m that is close to the T_m of SM isolated from natural sources (e.g., bovine brain SM (Barenholz et al., 1976)). SM is the most abundant sphingolipid in many tissues and in some cases the predominant phospholipid (e.g., the phospholipids content of the outer leaflet of the intestinal brush border membrane is ~75% SM and ~25% PC (Vénien and Le Grimellec, 1988)).

POPC was chosen to represent the low-melting component because it is a 1-saturated, 2-unsaturated PC, a common motif found in naturally occurring phospholipids, being the major lipid component in PC isolated from several natural sources (Marsh, 1990). It has a low T_m (Marsh, 1990), but it has the ability to form a lo phase in the presence of chol both below (Thewalt and Bloom, 1992) and above (Mateo et al., 1993) T_m, i.e., so/lo and ld/lo phase coexistence, respectively. It is used in several studies in ternary (or higher) model systems (e.g., Silvius, 1992; Milhiet et al., 2001; Dietrich et al., 2001). Recently, ld/lo phase separation in POPC/chol-oriented bilayers was detected by pulsed field gradient NMR (Lindblom et al., 2003).

Regarding the PSM/POPC binary system (Fig. 2), there is an interesting feature: although the phase diagram is of the same kind of the DPPC/POPC mixture (perithetic), PSM mixes with POPC in a way closer to ideal than DPPC (Curatolo et al., 1985). Although chol can recognize and interact preferentially with SM in a laterally phase-separated system, it cannot do so when in a miscible bilayer system composed, e.g., of PSM and DMPC (Calhoun and Shipley, 1979). Thus, it may be that the tendency of PSM and POPC to phase separate in the fluid is relevant in this context. The phase coexistence boundaries at room temperature are in good agreement with SM/12-spin label-PC (Ahmed et al. 1997). Gandhavadi et al. (2002) found no phase separation for DOPC/bovine brain SM (7:3) at 20°C; in the PSM/POPC diagram of Fig. 1, this is very close to the liquidus line, there being no extensive phase separation.

For the binary systems POPC/chol (Fig. 5) and PSM/chol (Fig. 4), and many ternary compositions (Fig. 7), the x_{chol} necessary to attain a single lo phase is much higher than in well-known phase diagrams like those for DPPC/chol (Ipsen et al., 1987; Sankaram and Thompson, 1991) and even DMPC/chol (Mateo et al., 1993; Almeida et al., 1992). The significance of this result is that ld/lo phase separation is very likely to occur in cell membranes with 30–40% chol. In case that the phase diagram was like, e.g., DPPC/chol by Vist and Davis (1990), then a single lo phase would be present. In agreement with phase separation persisting to higher x_{chol}, DSC data for PC/chol and SM/chol show that the low enthalpy, low cooperativity transition endures up to x_{chol} ~0.50 almost independently of the system (Maulik and Shipley, 1996; McIntosh et al., 1992; McMullen et al., 1993). This has been interpreted as the ''melting'' of the chol-rich phase, i.e., the lo/ld transition. To be consistent with that interpretation, it must be accepted that this kind of phase coexistence does persist up to that x_{chol}, in agreement with Fig. 5 (POPC/chol) and Fig. 4 above T_m (PSM/chol). Further evidence was obtained from freeze-fracture micros-

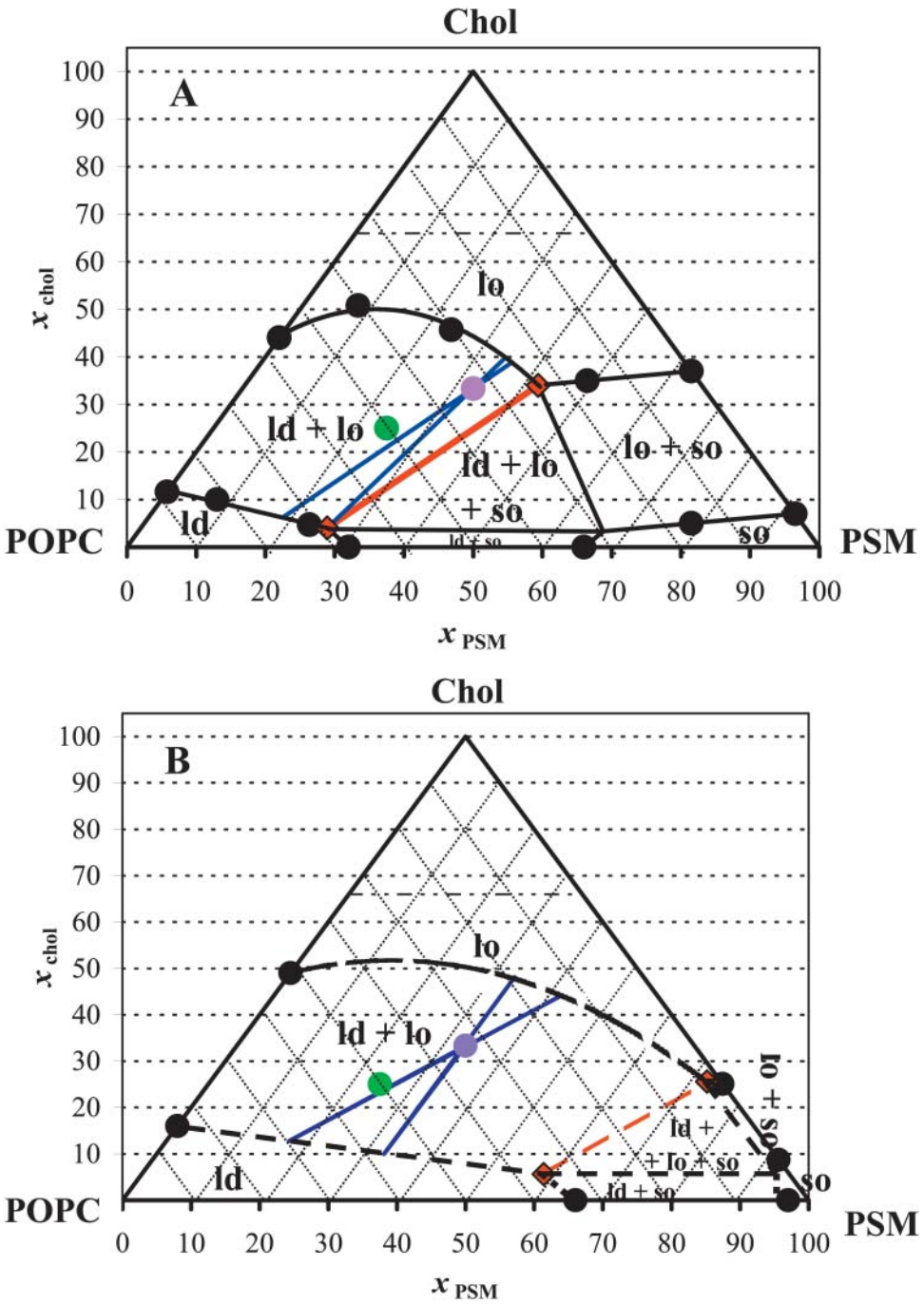

FIGURE 7 PSM/POPC/chol phase diagram at 23°C (*A*) and at 37°C (*B*). The circles are experimental points. The red (quasi) tie-line on the tie-triangle describes the lo/ld composition at the right of which there is also so phase. The blue tie-lines are the interval for the possible tie-lines that contain the 1:1:1 composition. The purple point marks the 1:1:1 composition and the green point marks the 2:1:1 composition. The phase boundaries for the diagram at 37°C are dashed lines to highlight the fact that no experimental determinations were performed for ternary mixtures at that temperature, due to technical limitations as described in the text. The dashed horizontal line for $x_{chol} = 0.66$ represents the cholesterol solubility limit on the lipid bilayer. The region above that line is of no interest for the present study because we are only interested in lamellar phases and it does not affect any of the conclusions. The value was chosen as the limit determined for several PC (Huang et al., 1999) at room temperature, but it should be noted that the value can be different for a lipid mixture, i.e., the line may not be horizontal, there can be temperature variations, and it was not determined for SM.

copy for DPPC/chol, e.g., at ~50°C, $x_{chol} \sim 0.45$, that suggests the existence of two phases that, on account of other data, are both fluid (Lentz et al., 1980). Recently, the phase boundaries for DPPC/chol and bovine brain SM were determined by ^{13}C-NMR, and both systems had a similar behavior, with an lo/ld phase coexistence persisting up to ~50% chol at 45°C (Guo et al., 2002).

The results obtained with ternary lipid mixtures, summarized in the phase diagrams of Fig. 7, are consistent with other literature works, namely detergent extraction data (e.g., Schroeder et al., 1994; Gandhavadi et al., 2002) and also AFM images, where phase separation can be undoubtedly observed for mixtures of bovine brain SM/POPC/chol (3:1:2) (Milhiet et al., 2001) and brain SM/DOPC/chol (1:1:1) with a predominance of the ordered domains (Yuan et al., 2002). For this last system (SM/DOPC), the presence of 10 mol % chol practically does not affect the monolayer topology, whereas it is strongly affected by 20% chol. The phase diagram at 23°C (Fig. 7 *A*) resembles the diagram DPPC/1-dodecanoyl-2-(12-bromododecanoyl)-PC/chol at

TABLE 1 Composition of conjugated ld/lo phases in ternary systems PC/SM/chol, at 23°C and 37°C

		ld			lo		
T (°C)	Tie-line	x_{PC}	x_{SM}	x_{chol}	x_{PC}	x_{SM}	x_{chol}
23	On tie-triangle	69	27	4	24	42	34
	Containing 1:1:1	74–69	19–27	6–4	25–26	36–35	39–40
37	On tie-triangle	36	59	6	1	73	26
	Containing 1:1:1	69–57	18–33	13–10	14–19	42–33	44–48
4	Containing 1:1:1	60	26	14	16	38	46
	Containing 8:1:1	81	10	9	57	18	25

SM is PSM and PC is POPC. The compositions given are the extremes of the tie-lines depicted in Fig. 7, *A* and *B*. At 4°C (results from Schroeder et al. (1994)), PC is from bovine liver and SM is from bovine brain, and lo is taken as the TX100 insoluble fraction and ld as the soluble fraction of the initial liposomes.

25°C (Silvius et al., 1996). It is interesting to note that the authors also considered so/lo coexistence for DPPC/chol present until ~38% chol (very near the value in the present study for PSM/chol) to obtain a consistent phase diagram, although the system should be completely in the lo phase at a much smaller x_{chol}, according to most of the published diagrams at the time.

From the ternary phase diagrams, it can be concluded that in plasma membranes with a high amount of chol and predominance of sphingolipids and lo forming PC-like POPC, the whole membrane can exist as a unique lo phase. This supports a previous proposal by Brown and London (1997). Also, according to those diagrams, at room temperature, for POPC/SM/chol (2:1:1) (*green point*, Fig. 7 *A*) there should be a considerable fraction of both ld and lo, but for a 1:1:1 ratio (*purple point*, Fig. 7 *A*), the lo phase should predominate, in agreement with other studies (Dietrich et al., 2001; Yuan et al., 2002). In fact, the ''raft mixtures'' in the work by Dietrich et al. (2001) have molar ratios 2:1:1 for the system POPC/SM/chol and 1:1:1 for DOPC/SM/chol. This is probably due to the fact, as explained below, that for the DOPC-containing system, the relative enrichment in SM when going from ld to lo along a tie-line is higher than for the POPC-containing systems, and the 1:1:1 composition should correspond to a more similar fraction of both phases, facilitating the domain visualization by the microscopy methods employed. In a recent AFM/DSC study, it was verified that SM/PC mixtures mimicking the outer leaflet of the brush border membrane displayed so/ld separation (Milhiet et al., 2002). As chol was added, the topology of the domains was changed (formation of lo domains), and eventually phase separation disappeared at high chol fractions. This behavior is what the diagrams in Fig. 7 predict. Usually three-phase coexistence areas are not observed, and there are many reasons for this, namely: i), one of the phases is present in a small amount; ii), there are small differences on physical properties between them; iii), the topology of the phases disguises one of them (Samsonov et al. (2001) do not discard the hypothesis of small so domains within the larger lo domains); iv), techniques sometimes do not distinguish ld from lo: e.g., wide-angle x-ray patterns (Gandhavadi et al., 2002); and v), techniques that do not distinguish so from lo (e.g., the photophysical data of *t*-PnA and DPH here described for PSM/chol mixtures below T_m).

Such as mentioned above, the main problems for the determination of a precise phase diagram are related to the sensitivity of the techniques. Curves like, e.g., $\langle r \rangle$ versus x_{chol} (Eq. 3 and Fig. 3 *A*) can have very subtle slope changes, making it difficult to determine precisely the beginning and ending of phase coexistence.

Why in fluorescence microscopy with ~33 mol % chol, two phases are seen in, e.g., DOPC/SM/chol (1:1:1) and not in, e.g., the binary mixtures POPC/chol (2:1) (Dietrich et al., 2001) or DPPC/chol (2:1) by AFM (Yuan and Johnston, 2001)? In the ternary system, the compositional difference between lo and ld phases is greater, and the properties of the coexisting phases may be more distinct and this may also allow for larger domains (in the optical microscopy experiment cited, 1 pixel corresponds to 80 nm). On another hand, the partition coefficient of the probes between the ordered and disordered phase in the ternary system can be further away from unity improving the ability to distinguish two phases, when present. In the case of DPPC/chol, the ''gel-like'' phase, if present (see, e.g., phase diagram in (Vist and Davis, 1990; Lentz et al., 1980), is in a too small amount to be detected. Thus, apart from the partition coefficients reasoning, if lipid rafts are to be considered as more ordered domains in an ld matrix, then the rafts region on the phase diagrams of Fig. 7 should exclude the upper part of the ld/lo phase coexistence, where the lo phase is predominant (and possibly includes a small portion of the tie-triangle, where the so phase represents only a very small fraction of the system, and the ld phase is predominant).

In quenching experiments (the quencher derivatized PC is the low-melting lipid), it is shown that $x_{chol} = 0.33$ promotes domain formation for a very large range of sphingolipid content at 37°C (Ahmed et al., 1997). This type of behavior is predicted by the hypothetical phase diagram of Fig. 7 *B* (except that phase separation occurs for 0% SM because the low-melting lipid used, POPC, has the ability to display ld/lo phase separation in the presence of chol, as previously mentioned). Although the lines drawn inside the diagram may not reflect quantitatively with high accuracy the

compositions of the coexisting phases, the overall phase behavior should be quite similar to that depicted in Fig. 7 *B*.

The directions of the tie-lines vary ''fanwise'' so that there is a gradual transition from the direction of one bounding tie-line to that of the other. No two tie-lines at the same temperature may ever cross. Beyond this, nothing can be said of their direction, except, of course, that they must connect liquidus to solidus. It is necessary, therefore, to determine the position and direction of the tie-lines by experiment and to indicate them on the ternary phase diagram (Rhines, 1956). It is common in the literature to find experiments performed on the lipid molar composition 1:1:1 (*purple points*, Fig. 7). The tie-line that crosses that composition can be approximated to a parallel to the red tie-line, on one extreme, or parallel to the POPC/chol side of the triangle, on the other extreme. But this last one would cross the tie-triangle at 23°C, so this reduces the uncertainty of that tie-line, because at the most, the tie-line is tangent to the triangle on the 100% ld vertex. This ''confidence interval'' is depicted in Fig. 7 *A* and the compositions presented in Table 1. The same calculations were performed with the hypothetical diagram for 37°C. In this case, both extreme directions were allowed, and the interval of compositions for ld and lo of lipid mixtures 1:1:1 is broader (Fig. 7 *B*, Table 1). The red quasi tie-line gives the compositions of the lipid mixtures for which PSM is most enriched but where there is a vanishing amount of so phase. When going from ld to lo along that line, the relative enrichment is higher for chol than for PSM. As shown in Table 1, at 37°C the composition of the coexisting lo and ld phases are more similar in terms of SM content than at lower temperatures (23°C). In cell membranes, other factors (e.g., the presence of proteins and/or phospholipids that cannot form a lo phase alone with chol at that temperature, as discussed below for DOPC) may increase the SM content of the rafts even at 37°C.

Detergent extraction at 4°C has been widely used, but this methodology is not consensual, as in fact we are in presence of a quaternary system. In this way, it is relevant to confront DRM composition with the compositions of the phases obtained from the diagrams here presented. The composition of the detergent-resistant and soluble fractions of PC/SM/chol liposomes obtained by Schroeder et al. (1994) at 4°C is shown in Table 1. Surprisingly, in the case of 1:1:1 liposomes, the compositions of these fractions are very similar to the lo and ld compositions taken from the diagram at 37°C. It should be stressed that the diagram at 4°C would be totally different, as concluded from the already noticeable differences between the diagrams obtained at 37°C and 23°C. It is then concluded that the detergent introduces a very strong perturbation, but by coincidence it reports a composition close to the one at 37°C. When starting from a 8:1:1 (PC:SM:chol) mixture, a different composition is obtained for the detergent soluble/insoluble fractions, but the soluble fraction has almost the same composition as the starting mixture (Table 1), and the insoluble fraction represents a very minor portion, and a high degree of uncertainty is associated to the values (Schroeder et al., 1994). The diagram at 37°C predicts that the 8:1:1 mixture should be completely on the ld phase, and according to the diagram at 23°C, only a very small amount should be in the lo phase, in agreement with detergent results. At 4°C, a POPC/PSM (8:1) contains ~10% of gel phase (Fig. 2).

The behavior of other lipidic systems, used as rafts models, can also be rationalized in the context of phase diagrams like those of Fig. 7. In the case of DOPC/brain SM/chol (1:1:1), no so phase was present at 20°C, as detected by x-ray diffraction, and detergent extraction at 4°C with 1% TX100 yields a DRM fraction with a composition very similar to the one in Table 1 (for 37°C), but the soluble fraction is much poorer in SM (<8%) and slightly richer in chol (19.6%) (Gandhavadi et al., 2002). This is because DOPC does not form lo phase and consequently the solubility of chol in ld is higher, at the expense of SM. Thus, the conjugated ld/lo compositional difference should be more pronounced in DOPC than in POPC containing liposomes. It is possible that this qualitative difference justifies the difficulty in observing raft-like domains in POPC-containing mixtures as compared to DOPC. In fact, if the compositional difference is less pronounced, it is also expected that the physical properties (e.g., bilayer thickness) are also more similar, and namely the partition coefficients of probes and their fluorescence parameters are less well differentiated. Nevertheless, from our point of view, models containing POPC are biologically more relevant than those containing DOPC as the low melting lipid. It is worth mentioning that in many studies, egg PC is used, which is very rich in POPC (Marsh, 1990).

Some other literature results may be explained by the coexistence of three phases. The quenching of DPH fluorescence in liposomes PSM/doxyl-PC (1:1) is effective both above and below T_m of PSM (Kuikka et al., 2001). The introduction of 15 mol % chol decreases the extent of quenching, especially below T_m, where a gel/fluid phase separation occurs in the absence of chol (Ahmed et al., 1997). Usually the decrease in quenching in this type of experiments is interpreted as the appearance of domains (phase separation) from a previously homogeneous system. In the case of the experiment by Kuikka et al. (2001), once that phase separation already existed, this result is best interpreted if a coexistence of three phases is considered in the presence of chol, maximizing the segregation of probe and quencher. Another literature result that can be tentatively explained is the AFM study by Milhiet et al. (2001). The decrease in height difference between ''light'' and ''dark'' domains in SM/POPC monolayers with increasing x_{chol} can be interpreted as follows: initially ''so/ld'' phase separation occurs; with the addition of chol, lo domains start to form, but there is persistence of so-like domains; with the addition of a certain amount of chol, the so-like domains disappear, i.e., the system is in the lo/ld phase coexistence region, with

a height difference smaller than for so/ld; finally, with a sufficiently large fraction of chol, all the monolayer is in the lo phase (no height differences). These changes are not along a tie-line, and thus the phase types and their respective compositions vary.

Although several different techniques and distinct model systems have been employed with the purpose of modeling lipid rafts, which resulted in a significant amount of data often difficult to conciliate, many of the apparent contradictions between them seem to point, after all, to the same general behavior.

It should be stressed that, as well as for binary, for ternary systems the determination of partition constants for probes (e.g., rafts markers) should be made along a tie-line. Only along such a line the phase compositions are kept constant. At present, we are carrying out topological studies using FRET according to a methodology previously applied to binary systems (Loura et al., 2001, 2000) and for which the knowledge of the tie-lines is required. The size of the domains for low lo fraction is very small, below optical resolution (unpublished FRET data). In the context of rafts, they should also be considered, because several studies in cell membranes suggest that rafts, if present, may have size below optical resolution (Anderson and Jacobson, 2002).

This highlights the complementarity and the importance of using different methodologies in the raft field. In the near future, it will be interesting to confront the phase diagrams here presented with those obtained by different techniques and on different model systems, e.g., microscopy (Smith et al., 2003) and fluorescence correlation spectroscopy (Kahya et al., 2003) on giant unilamellar vesicles.

It is shown here that if rafts in cell membranes are lo-like domains, these can have multiple compositions (reflected in different size, topology, and dynamics). On other words, there is no ''magical'' raft mixture. The region of the diagram where rafts (lo phase domains) have a more defined size, topology and dynamics can be narrowed down to a much less extensive region, but the composition of the coexisting phases is still given by the extreme of the tie-lines, and the phase diagrams will be always indispensable tools.

Dr. Luís M.S. Loura is acknowledged for helpful discussions.

This material was presented in part at the COST D22 1st Domain Working Group Meeting (Segovia, Spain, June, 2002) and at the 47th Biophysical Society Annual Meeting (San Antonio, TX, March 2003). This work and research grants (A.F. and R.F.M. de A.) were supported by POCTI (Fundação para a Ciência e a Tecnologia), Portugal.

REFERENCES

Ahmed, S. N., D. A. Brown, and E. London. 1997. On the origin of sphingolipid/cholesterol-rich detergent-insoluble cell membranes: physiological concentrations of cholesterol and sphingolipid induce formation of a detergent-insoluble, liquid-ordered lipid phase in model membranes. *Biochemistry*. 36:10944–10953.

Almeida, P. F. F., W. L. C. Vaz, and T. E. Thompson. 1992. Lateral diffusion in the liquid phases of dimyristoylphosphatidylcholine/cholesterol lipid bilayers: a free volume analysis. *Biochemistry*. 31:6739–6747.

Anderson, R. G. W., and K. Jacobson. 2002. A role for lipid shells in targeting proteins to caveolae, rafts and other lipid domains. *Science*. 296:1821–1825.

Barenholz, Y., J. Suurkuusk, D. Mountcastle, T. E. Thompson, and R. L. Biltonen. 1976. A calorimetric study of the thermotropic behavior of aqueous dispersions of natural and synthetic sphingomyelins. *Biochemistry*. 15:2441–2447.

Brown, D. A., and E. London. 1997. Structure of detergent-resistant membrane domains: does phase separation occur in biological membranes? *Biochem. Biophys. Res. Commun*. 240:1–7.

Calhoun, W. I., and G. G. Shipley. 1979. Sphingomyelin-lecithin bilayers and their interaction with cholesterol. *Biochemistry*. 18:1717–1722.

Curatolo, W., B. Sears, and L. J. Neuringer. 1985. A calorimetry and deuterium NMR study of mixed model membranes of 1-palmitoyl-2-oleylphosphatidylcholine and saturated phosphatidylcholines. *Biochim. Biophys. Acta*. 817:261–270.

de Almeida, R. F. M., L. M. S. Loura, A. Fedorov, and M. Prieto. 2002. Nonequilibrium phenomena in the phase separation of a two-component lipid bilayer. *Biophys. J*. 82:823–834.

Dietrich, C., L. A. Bagatolli, Z. N. Volovyk, N. L. Thompson, M. Levi, K. Jacobson, and E. Gratton. 2001. Lipid rafts reconstituted in model membranes. *Biophys. J*. 80:1417–1428.

Epand, R. M., and M. A. Moscarello. 1982. The effects of bovine myelin basic protein on the phase transition properties of sphingomyelin. *Biochim. Biophys. Acta*. 685:230–232.

Estep, T. N., D. B. Mountcastle, Y. Barenholz, R. L. Biltonen, and T. E. Thompson. 1979. Thermal behavior of synthetic sphingomyelin-cholesterol dispersions. *Biochemistry*. 18:2112–2117.

Feigenson, G. W., and T. Buboltz. 2001. Ternary phase diagram of dipalmitoyl-PC/dilauroyl-PC/cholesterol: nanoscopic domain formation driven by cholesterol. *Biophys. J*. 80:2775–2788.

Gandhavadi, M., D. Allende, A. Vidal, S. A. Simon, and T. J. McIntosh. 2002. Structure, composition, and peptide binding properties of detergent soluble bilayers and detergent resistant rafts. *Biophys. J*. 82:1469–1482.

Guo, W., V. Kurze, T. Huber, N. H. Afdhal, K. Beyer, and J. A. Hamilton. 2002. A solid-state NMR study of phospholipid-cholesterol interactions: sphingomyelin-cholesterol binary systems. *Biophys. J*. 83:1465–1478.

Heerklotz, H. 2002. Triton promotes domain formation in lipid raft mixtures. *Biophys. J*. 83:2693–2701.

Huang, J., J. T. Buboltz, and G. W. Feigenson. 1999. Maximum solubility of cholesterol in phosphatidylcholine and phosphatidylethanolamine bilayers. *Biochim. Biophys. Acta*. 1417:89–100.

Ipsen, J. H., G. Karlström, O. G. Mouritsen, H. Wennerström, and M. J. Zuckermann. 1987. Phase equilibria in the phosphatidylcholine-cholesterol system. *Biochim. Biophys. Acta*. 905:162–172.

Kahya, N., D. Scherfeld, K. Bacia, B. Poolman, and P. Schwille. 2003. Probing lipid mobility of raft-exhibiting model membranes by fluorescence correlation spectroscopy. *J. Biol. Chem*. 28109–28815.

Koynova, R., and M. Caffrey. 1995. Phases and phase transitions of the hydrated sphingolipids. *Biochim. Biophys. Acta*. 1255:213–236.

Koynova, R., and M. Caffrey. 1998. Phases and phase transitions of the phosphatidylcholines. *Biochim. Biophys. Acta*. 1376:91–145.

Kuikka, M., H. O.-R. Ramstedt, J. Tuuf, and J. P. Slotte. 2001. Membrane properties of D-erythro-*N*-acyl sphingomyelins and their corresponding dihydro species. *Biophys. J*. 80:2327–2337.

Lakowicz, J. R. 1999. Principles of Fluorescence Spectroscopy, 2nd ed. Kluwer/Plenum, New York.

Lentz, B. R. 1988. Membrane ''fluidity'' from fluorescence anisotropy measurements. *In* Spectroscopic Membrane Probes, Vol. I. L. M. Loew, editor. CRC, Boca Raton, FL. 13–41.

Lentz, B. R., Y. Barenholz, and T. E. Thompson. 1976a. Fluorescence depolarization studies of phase transitions and fluidity in phospholipid

bilayers. 1. Single component phosphatidylcholine liposomes. *Biochemistry*. 15:4521–4528.

Lentz, B. R., Y. Barenholz, and T. E. Thompson. 1976b. Fluorescence depolarization studies of phase transitions and fluidity in phospholipid bilayers. 2 Two-component phosphatidylcholine liposomes. *Biochemistry*. 15:4529–4537.

Lentz, B. R., D. A. Barrow, and M. Hoechli. 1980. Cholesterol-phosphatidylcholine interactions in multilamellar vesicles. *Biochemistry*. 19:1943–1954.

Lindblom, G., A. Filippov, and G. Oradd. 2003. The effect of cholesterol on the lateral diffusion of phospholipids in oriented bilayers. *Biophys. J*. 84:378a.

London, E., and D. A. Brown. 2000. Insolubility of lipids in triton X-100: physical origin and relationship to sphingolipid/cholesterol membrane domains (rafts). *Biochim. Biophys. Acta*. 1508:182–195.

Loura, L. M. S., A. Fedorov, and M. Prieto. 2000. Partition of membrane probes in a gel/fluid two-component lipid system: a fluorescence resonance energy transfer study. *Biochim. Biophys. Acta*. 1467:101–112.

Loura, L. M. S., A. Fedorov, and M. Prieto. 2001. Fluid-fluid membrane microheterogeneity: a fluorescence resonance energy transfer study. *Biophys. J*. 80:776–788.

Mabrey, S., and J. M. Sturtevant. 1976. Investigation of phase transitions of lipids and lipid mixtures by high-sensitivity differential scanning calorimetry. *Proc. Natl. Acad. Sci. USA*. 73:3862–3866.

Marsh, D. 1990. Handbook of Lipid Bilayers. CRC, Boca Raton, FL.

Mateo, C. R., J.-C. Brochon, M. P. Lillo, and A. U. Acuña. 1993. Liquid-crystalline phases of cholesterol/lipid bilayers as revealed by the fluorescence of *trans*-parinaric acid. *Biophys. J*. 65:2237–2247.

Maulik, P. R., and G. G. Shipley. 1996. *N*-palmitoyl sphingomyelin bilayers: structure and interactions with cholesterol and dipalmitoylphosphatidylcholine. *Biochemistry*. 35:8025–8034.

McClare, C. W. F. 1971. An accurate and convenient organic phosphorus assay. *Anal. Biochem*. 39:527–530.

McIntosh, T. J., S. A. Simon, D. Needham, and C.-H. Huang. 1992. Structure and cohesive properties of sphingomyelin/cholesterol bilayers. *Biochemistry*. 31:2012–2020.

McMullen, T. P. W., R. N. A. H. Lewis, and R. N. McElhaney. 1993. Differential scanning calorimetric study of the effect of cholesterol on the thermotropic phase behavior of a homologous series of linear saturated phosphatidylcholines. *Biochemistry*. 32:516–522.

McMullen, T. P. W., and R. N. McElhaney. 1995. New aspects of the interaction of cholesterol with dipalmitoylphosphatidylcholine bilayers as revealed by high-sensitivity differential scanning calorimetry. *Biochim. Biophys. Acta*. 1234:90–98.

Milhiet, P. E., C. Domec, M.-C. Giocondi, N. Van Mau, F. Heitz, and C. Le Grimellec. 2001. Domain formation in models of the renal brush border membrane outer leaflet. *Biophys. J*. 81:547–555.

Milhiet, P. E., M.-C. Giocondi, and C. Le Grimellec. 2002. Cholesterol is not crucial for the existence of microdomains in kidney brush-border membrane models. *J. Biol. Chem*. 277:875–878.

Rhines, F. N. 1956. Phase Diagrams in Metallurgy: Their Development and Application. McGraw-Hill, New York.

Samsonov, A. V., I. Mihalyov, and F. S. Cohen. 2001. Characterization of cholesterol-sphingomyelin domains and their dynamics in bilayer membranes. *Biophys. J*. 81:1486–1500.

Sankaram, M. B., and T. E. Thompson. 1990. Interaction of cholesterol with various glycerophospholipids and sphingomyelin. *Biochemistry*. 29:10670–10675.

Sankaram, M. B., and T. E. Thompson. 1991. Cholesterol-induced fluid-phase immiscibility in membranes. *Proc. Natl. Acad. Sci. USA*. 88:8686–8690.

Santos, N. C., M. Prieto, and M. A. R. B. Castanho. 1998. Interaction of the major epitope region of HIV protein gp41 with membrane model systems. A fluorescence spectroscopy study. *Biochemistry*. 37:8674–8682.

Schroeder, R., S. A. Ahmed, Y. Zhu, E. London, and D. Brown. 1998. Cholesterol and sphingolipid enhance the Triton X-100 insolubility of glycosylphosphatidylinositol-anchored proteins by promoting the formation of detergent-insoluble ordered membrane domains. *J. Biol. Chem*. 273:1150–1157.

Schroeder, R., E. London, and D. Brown. 1994. Interactions between saturated acyl chains confer detergent resistance on lipids and glycosylphosphatidylinositol (GPI)-anchored proteins: GPI-anchored proteins in liposomes and cells show similar behavior. *Proc. Natl. Acad. Sci. USA*. 91:12130–12134.

Silvius, J. R. 1992. Cholesterol modulation of lipid intermixing in phospholipid and glycosphingolipid mixtures. Evaluation using fluorescent lipid probes and brominated lipid quenchers. *Biochemistry*. 31: 3398–3408.

Silvius, J. R., D. del Giudice, and M. Lafleur. 1996. Cholesterol at different bilayer concentrations can promote or antagonize lateral segregation of phospholipids of differing acyl chain length. *Biochemistry*. 35:15198–15208.

Simons, K., and E. Ikonen. 1997. Functional rafts in cell membranes. *Nature*. 387:569–572.

Sklar, L. A., B. S. Hudson, M. Petersen, and J. Diamond. 1977b. Conjugated polyene fatty acids on fluorescent probes: spectroscopic characterization. *Biochemistry*. 16:813–818.

Sklar, L. A., B. S. Hudson, and R. D. Simoni. 1977a. Conjugated polyene fatty acids as fluorescent probes: synthetic phospholipid membrane studies. *Biochemistry*. 16:819–828.

Sklar, L. A., G. P. Miljanich, and E. A. Dratz. 1979. Phospholipid lateral phase separation and the partition of *cis*-parinaric acid and *trans*-parinaric acid among aqueous, solid lipid, and fluid lipid phases. *Biochemistry*. 18:1707–1716.

Smith, A. K., J. Buboltz, C. H. Spink, and G. W. Feigenson. 2003. Ternary phase diagram of the lipid mixture sphingomyelin/DOPC/cholesterol. *Biophys. J*. 84:372a.

Sot, J., M. I. Collado, J. L. R. Arrondo, A. Alonso, and F. M. Goñi. 2002. Triton X-100 resistant bilayers: effect of lipid composition and relevance to the raft phenomenon. *Langmuir*. 18:2828–2835.

Thewalt, J. L., and M. Bloom. 1992. Phosphatidylcholine: cholesterol phase diagrams. *Biophys. J*. 63:1176–1181.

Vénien, C., and C. Le Grimellec. 1988. Phospholipid asymmetry in renal brush-border membranes. *Biochim. Biophys. Acta*. 942:159–168.

Vist, M. R., and J. H. Davis. 1990. Phase equilibria of cholesterol/dipalmitoylphosphatidylcholine mixtures: ^{2}H nuclear magnetic resonance and differential scanning calorimetry. *Biochemistry*. 29:451–464.

Wardlaw, J. R., W. H. Sawyer, and J. P. Ghiggino. 1987. Vertical fluctuations of phospholipid acyl chains in bilayers. *FEBS Lett*. 223:20–24.

Xu, X., and E. London. 2000. The effect of sterol structure on membrane lipid domains reveals how cholesterol can induce lipid domain formation. *Biochemistry*. 39:843–849.

Yuan, C., J. Furlong, P. Burgos, and L. J. Johnston. 2002. The size of lipid rafts: an atomic force microscopy study of ganglioside GM1 domains in sphingomyelin/DOPC/cholesterol membranes. *Biophys. J*. 82:2526–2535.

Yuan, C., and L. J. Johnston. 2001. Atomic force microscopy studies of ganglioside GM1 domains in phosphatidylcholine and phosphatidylcholine/cholesterol bilayers. *Biophys. J*. 81:1059–1069.

Yuann, J. M., and R. D. Morse. 1999. Determination by photoreduction of flip-flop kinetics of spin-labeled stearic acids across phospholipid bilayers. *Biochim. Biophys. Acta*. 1416:135–144.